Dynamics of a Receptor-Bound Ligand by Heteronuclear NMR: FK506 Bound to FKBP-12

Christopher A. Lepre,* Jya-Wei Cheng, and Jonathan M. Moore

Vertex Pharmaceuticals, Incorporated 40 Allston Street, Cambridge, Massachusetts 02139-4211

Received March 8, 1993

FK506 is a potent immunosuppressant that inhibits T-cell activation by blocking early steps in cytoplasmic signal transduction.[1] The complex formed by FK506 and its major binding protein, FKBP-12, binds and inhibits the activity of calcineurin (CN), a Ca^{+2}-dependent phosphatase proposed to be the cellular target of FK506.[2-6] Although structural data are unavailable for the FK506/FKBP/CN complex, studies involving chemical modifications of FK506 and mutations of FKBP-12[6-9] have shown that the solvent-exposed portion of FK506 and nearby FKBP-12 residues are essential for CN inhibition. This important region of the FK506/FKBP-12 complex has been difficult to characterize structurally since it makes intermolecular contacts in crystals[10,11] and is partly disordered in NMR solution structures.[12] In this work, 2D inverse-detected ^{13}C NMR relaxation methods developed recently for measuring protein dynamics have been used to study the mobility of ^{13}C-labeled FK506 bound to human recombinant FKBP-12. The results reveal that the ligand is unexpectedly rigid in regions of the drug that are highly exposed to solvent and, as the first application of inverse-detected ^{13}C NMR relaxation methods to a receptor-bound drug, demonstrate the general utility of these new techniques in structure-based drug design.

The ^{13}C T_1 and NOE relaxation parameters for the methine sites of ^{13}C-labeled FK506 were determined, respectively, from two-dimensional sensitivity-enhanced proton-detected inversion–recovery and steady-state $\{^1H\}$-^{13}C NOE experiments.[13,14] T_2 relaxation data were not used due to interference by carbon–carbon couplings, which are the result of the high level of isotopic enrichment present in the sample.

Longitudinal relaxation rates (R_1) were obtained by nonlinear least-squares fitting of the T_1 experimental peak intensities to a single three-term exponential, as described by Palmer et al.[15] The relaxation data (Table I) were interpreted by using the model-free formalism of Lipari and Szabo.[16,17] Since T_2 data were unavailable, it was necessary to make an initial estimate of the overall molecular correlation time, $\tau_m = 6$ ns, by assuming that all internal motions were fast (less than 20 ps). To calculate the model-free parameters, the spectral density function for the motions of the C–H bond vectors was represented by

$$J(w) = {}^2/_5\left[\frac{S^2\tau_m}{1+(\omega\tau_m)^2} + \frac{(1-S^2)\tau}{1+(\omega\tau)^2}\right]$$

where S^2 is the generalized order parameter reflecting the amplitude of the motions and $\tau^{-1} = \tau_m^{-1} + \tau_e^{-1}$, where τ_m is the overall correlation time (6 ns) and τ_e is the effective correlation time for local motions.[16] The calculations of S^2, τ_e, and their

Table I. Relaxation Data and Calculated Model-Free Parameters for ^{13}C-FK506 Bound to FKBP-12[a]

site[b]	R_1[c]	NOE[d]	R_{1p}[e]	S^2[f]	τ_e[g]
11-CH	1.62(0.04)	1.164[h]	0.65	0.87(0.07)	1.4(0.1)
12-CH_2			0.88, 0.47		
13-CH	1.57(0.03)	1.214(0.005)	0.94	0.82(0.07)	12.2(0.9)
14-CH	1.40(0.03)	1.207(0.017)	1.16	0.74(0.07)	6.4(1.8)
15-CH	1.44(0.03)	1.182[h]	0.91	0.77(0.06)	3.5(1.1)
16-CH_2			0.66, 0.85		
17-CH	1.70(0.04)	1.302(0.015)	*i*	0.85(0.07)	41.5(3.3)
18-CH_2			0.91[j]		
21-CH	1.58(0.04)	1.221(0.014)	2.22	0.83(0.05)	14.4(1.4)
23-CH_2			1.65, 1.96		
24-CH	1.45(0.03)	1.207(0.009)	1.73	0.76(0.06)	7.3(0.6)
25-CH	1.55(0.04)	1.204(0.054)	1.14	0.82(0.07)	9.6(0.6)
26-CH	1.67(0.04)	1.192(0.005)	0.80	0.88(0.07)	12.0(1.2)
28-CH	*i*		1.11		
29-CH	*i*		1.23		
30-CH_2			0.72, 1.07		
31-CH	1.07(0.03)	1.163(0.003)	1.33	0.58(0.08)	0.2(0.3)
32-CH	1.04(0.03)	1.265(0.008)	1.70	0.53	5.9(0.6)
33-CH_2			1.78, 2.08		
34-CH_2			1.41[j]		
11-Me			0.20		
35-CH_2			1.13, 1.22[k]		
36-CH	0.21	*i*	2.13	0.11[l]	0[l]
37-CH_2			1.94, 2.06[m]		
25-Me			0.72		
27-Me			1.04		
13-OMe			1.18		
15-OMe			1.27		
31-OMe			1.01		

[a] All data were collected on a Bruker AMX-500 spectrometer at 303 K using a sample of 2.8 mM 1:1 complex in 50 mM potassium phosphate/D_2O at pD 7.4 (see ref 12). [b] Modified Cambridge Data Base numbering. [c] Longitudinal relaxation rate in units of s^{-1}, with standard deviations (parenthesized) determined by the method of ref 15. Thirteen inversion–recovery spectra were recorded for T = 10, 20, 51, 102, 153, 203, 254, 305, 356, 407, 509, 712, and 814 ms with a 2.5-s relaxation delay. [d] Heteronuclear NOEs are taken as the ratio of peak heights in spectra acquired with and without proton saturation. Two independent data sets were acquired as described in ref 13, with a 4.0-s relaxation delay. Mean values and standard errors reported are from the two independent data sets. [e] Paramagnetic contribution to the proton relaxation rate, in units of s^{-1}. For pairs of methylene protons, the *pro-R* proton is listed first. Rates were determined from three-parameter linear least-squares fits of peak intensities from 2D inversion–recovery HMQC spectra.[20] Seven to ten spectra were collected with delays from 0 to 1500 ms, with a relaxation delay of 2.5 s. [f] Generalized order parameter (dimensionless) calculated by minimizing the squares of the differences between the experimental and back-calculated R_1 and NOE values (see ref 15). CSA contributions to the relaxation were not included. [g] Effective correlation time for local motions, in units of ps. [h] NOE value from one data set. [i] Not determined. [j] *pro-R* proton only. [k] Not stereospecifically assigned. [l] Calculated by assuming that internal motion is very fast ($\tau_e < 10$ ps). [m] Values for *cis*, *trans* protons.

(1) Reviews: Schreiber, S. L. *Science* **1991**, *251*, 283–287; Rosen, M. K.; Schreiber, S. L. *Angew. Chem., Int. Ed. Eng.* **1992**, *31*, 384–400. Schreiber, S. L.; Liu, J.; Albers, M. W.; Rosen, M. W.; Standaert, R. F.; Wandless, T. J.; Somers, P. K. *Tetrahedron* **1992**, *48*, 2545–2558. Sigal, N. H.; Dumont, F. J. *Annu. Rev. Immunol.* **1992**, *10*, 519–60.

(2) Liu, J.; Farmer, J. D.; Lane, W. S.; Friedman, J.; Weissman, I.; Schreiber, S. L. *Cell* **1991**, *66*, 807–815.

(3) Fruman, D. A.; Klee, C. B.; Bierer, B. E.; Burakoff, S. J. *Proc. Natl. Acad. Sci. U.S.A.* **1992**, *89*, 3686–3690.

(4) O'Keefe, S. J.; Tamura, J.; Kincaid, R. L.; Tocci, M. J.; O'Neill, E. A. *Nature* **1992**, *357*, 692–694.

(5) Clipstone, N. A.; Crabtree, G. R. *Nature* **1992**, *357*, 695–697.

(6) Liu, J.; Albers, M. W.; Wandless, T. J.; Luan, S.; Alberg, D. G.; Belshaw, P. J.; Cohen, P.; MacKintosh, C.; Klee, C. B.; Schreiber, S. L. *Biochemistry* **1992**, *31*, 3896–3901.

(7) Aldape, R. A.; Futer, O.; DeCenzo, M. T.; Jarrett, B. P.; Murcko, M. A.; Livingston, D. J. *J. Biol. Chem.* **1992**, *267*, 16029–16032.

(8) Yang, D.; Rosen, M. K.; Schreiber, S. L. *J. Am. Chem. Soc.* **1993**, *115*, 819–820.

(9) Rosen, M. K.; Yang, D.; Martin, P. K.; Schreiber, S. L. *J. Am. Chem. Soc.* **1993**, *115*, 821–822.

(10) Van Duyne, G. D.; Standaert, R. F.; Karplus, P. A.; Schreiber, S. L.; Clardy, J. *Science* **1991**, *252*, 839–842.

(11) Yamashita, M. M.; Rotstein, S. H.; Murcko, M. M.; Wilson, K.; Boger, J.; Thomson, J. A.; Fitzgibbon, M. J.; Navia, M. A., unpublished results.

(12) Lepre, C. A.; Thomson, J. A.; Moore, J. M. *FEBS Lett.* **1992**, *302*, 89–96.

(13) Kördel, J.; Skelton, N. J.; Akke, M.; Palmer, A. G.; Chazin, W. J. *Biochemistry* **1992**, *31*, 4856–4866.

(14) Stone, M. J.; Fairbrother, W. J.; Palmer, A. G.; Reizer, J.; Saier, M. H.; Wright, P. E. *Biochemistry* **1992**, *31*, 4394–4406.

(15) Palmer, A. G.; Rance, M.; Wright, P. E. *J. Am. Chem. Soc.* **1991**, *113*, 4371–4380.

(16) Lipari, G.; Szabo, A. *J. Am. Chem. Soc.* **1982**, *104*, 4546–4559.

(17) Lipari, G.; Szabo, A. *J. Am. Chem. Soc.* **1982**, *104*, 4559–4570.

0002-7863/93/1515-4929$04.00/0

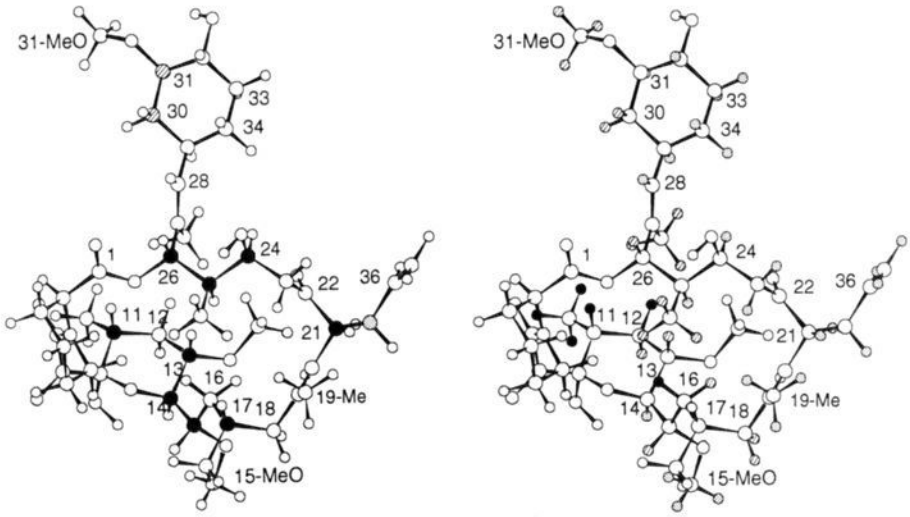

Figure 1. Stereoview of FK506 with atoms shaded to show the dynamics and solvent exposure results. (Left) Carbons shaded according to the following scheme: dot pattern, $S^2 < 0.50$; hatched, $0.50 < S^2 < 0.70$; black, $S^2 > 0.70$; white, no data. (Right) Protons shaded according to the following scheme: dot pattern, $R_{1\rho} > 1.10$; hatched, $0.70 < R_{1\rho} < 1.10$; black, $R_{1\rho} < 0.70$; white, no data.

uncertainties from R_1 and NOE data were carried out essentially as described by Palmer et al.[15] In order to check the initial estimated τ_m value (6 ns), τ_m was back-calculated by assigning a value of $S^2 = 0.88$ (the average S^2 for backbone amides of FK506/FKBP-12[18]) to four deeply buried sites that were expected to have the lowest mobility. The back-calculated τ_m was 6.2 ns, indicating that the estimated value is a good approximation, and the values for τ_e were less than 20 ps, verifying that the initial assumption of $\tau_e \approx 0$ is valid for these sites. The validity of the initial approximation was further confirmed by comparing the predicted and experimental values of R_1 as a function of τ_e: the best agreement between predicted and observed R_1 values was found for $\tau_e \approx 0$.

The solvent exposure of proton sites in bound FK506 was determined by measuring the change in proton T_1 relaxation rates caused by adding 5 mM HyTEMPO, a noncoordinating paramagnetic probe.[19,20] The paramagnetic contribution to the longitudinal relaxation rate ($R_{1\rho}$, Table I) is largest for protons with the greatest exposure to solvent. As shown in Figure 1, the regions of bound FK506 that are most solvent-exposed are the allyl group, the macrocycle back-bone from 19-Me to C25, and the C32–C33 edge of the cyclohexyl ring.

The dynamics results indicate that the macrocycle backbone of bound FK506 is relatively immobile on the picosecond time scale. Interestingly, this includes the C21 and C25 sites (order parameters $S^2 = 0.83$ and 0.82, respectively) which are located on a loop that extends out from the protein surface[10,11] and is highly exposed to solvent (Figure 1). For comparison, the deeply buried pyranose ring exhibits NOEs to side chains in the FKBP-12 binding pocket,[12] shows the lowest degree of solvent exposure (Table I), and has sites with order parameters $S^2 = 0.82$ and 0.87 (C13 and C11). Thus, for these sites on the macrocycle, high solvent exposure is not associated with higher mobility. The low mobility of the C21–C25 region need not be a consequence of protein binding because the macrocycle is inherently constrained; unrestrained MD simulations show that, even in the free ligand, macrocycle motions on the subnanosecond time scale are conformationally hindered.[21,22] It is interesting to note that S^2 is slightly lower at C14 and C15 (0.74, 0.77) than at the rest of the backbone sites (mean $S^2 = 0.83 \pm 0.04$). These sites adjoin 15-OMe, which lies exposed in a cleft near the side chains of D37 and R42; this composite ligand–protein surface is reportedly involved in calcineurin inhibition by FK506/FKBP-12.[6-8]

In other regions of the ligand, mobility is correlated with higher solvent exposure. For example, the solvent exposed allyl group is highly disordered. During refinement of the NMR structure of bound FK506, regions of the ligand that were poorly defined by constraints adopted conformations that were dictated by the force field of the free ligand.[12] The present dynamics results confirm that, as expected, the allyl group is disordered even though it appears to be localized in the refined NMR structures. Similarly, the well-defined conformation of the ethyl group of ascomycin in its FKBP-12 complex[23] may also be an artifact of the refinement process, since it occupies the same location as the allyl of FK506 and hence should be highly disordered.

The exocyclic cyclohexyl group is exposed to solvent along one edge: $R_{1\rho}$ for 32-CH and 33-CH_2 is roughly twice that of 30-CH_2 and 31-MeO, in agreement with X-ray[10,11] and NMR[12] results showing that the latter sites contact the protein. This exposure pattern indicates that rotation about the C28–C29 bond is hindered, which is consistent with the results of unrestrained MD simulations of free FK506.[21,22] The order parameters for C30 and C31 on the cyclohexyl are lower than measured for the macrocycle but are not as low as observed for the allyl group.

The low flexibility of certain solvent-exposed regions of FK506 suggests that the successful design of compounds to mimic its activity may require structural rigidity in the functional groups designed to interact with calcineurin. Thus, NMR relaxation methods offer information for drug design that is unavailable from other structural methods which provide static models of bound ligands.

Acknowledgment. ^{13}C-FK506 was produced by H. Kuboniwa and K. Munemura of Chugai Pharmaceuticals, Inc. using a germline kindly provided by K. Nagai at Tokyo Institute of Technology. We are indebted to S. Chambers for overexpressing FKBP-12, M. Fitzgibbon and J. Black for purifying the protein, and J. Thomson for preparing the complex. We wish to thank A. Palmer for providing data analysis programs and useful discussions, as well as D. Pearlman and J. Griffith for software assistance. Lastly, we acknowledge the assistance of M. Rance with the experimental techniques.

(18) Cheng, J.-W.; Lepre, C. A.; Chambers, S. P.; Fulghum, J. R.; Moore, J. M., unpublished results.

(19) Niccolai, N.; Valensin, G.; Rossi, C.; Gibbons, W. A. *J. Am. Chem. Soc.* **1982**, *104*, 1534–1537.

(20) Petros, A. M.; Neri, P.; Fesik, S. W. *J. Biomolec. NMR* **1992**, *2*, 11–18.

(21) Pranata, J.; Jorgensen, W. L. *J. Am. Chem. Soc.* **1991**, *113*, 9483–9493.

(22) Pearlman, D. A., submitted for publication.

(23) Meadows, R. P.; Nettesheim, D. G.; Xu, R. X.; Olejniczak, E. T.; Petros, A. M.; Holzman, T. F.; Severin, J.; Gubbins, E.; Smith, H.; Fesik, S. W. *Biochemistry* **1993**, *32*, 754–765.